Topographically selective atomic layer deposition within trenches enabled by an amorphous carbon inhibition layer

Thijs Janssen ; Lodewijk J. P. Vossen ; Marcel A. Verheijen ; Wilhelmus M. M. Kessels ; Adriaan J. M. Mackus ✉

Check for updates

View Online   Export Citation

Articles You May Be Interested In

Atomic layer deposition and selective etching of ruthenium for area-selective deposition: Temperature dependence and supercycle design

J. Vac. Sci. Technol. A (April 2021)

Homogeneous high In content $In_xGa_{1-x}N$ films by supercycle atomic layer deposition

J. Vac. Sci. Technol. A (November 2022)

Conformal deposition of GeTe films with tunable Te composition by atomic layer deposition

J. Vac. Sci. Technol. A (January 2019)

Applied Physics Letters

Topographically selective atomic layer deposition within trenches enabled by an amorphous carbon inhibition layer

View Online   Export Citation   CrossMark

Thijs Janssen,[1] (iD) Lodewijk J. P. Vossen,[1] (iD) Marcel A. Verheijen,[1,2] (iD) Wilhelmus M. M. Kessels,[1] (iD)
and Adriaan J. M. Mackus[1,a] (iD)

AFFILIATIONS

[1]Department of Applied Physics, Eindhoven University of Technology, P. O. Box 513, 5600 MB Eindhoven, The Netherlands
[2]Eurofins Materials Science BV, High Tech Campus, Eindhoven 5656AE, The Netherlands

[a]Author to whom correspondence should be addressed: a.j.m.mackus@tue.nl

ABSTRACT

To meet the demands for more advanced computer chips, creating devices with advanced 3D architectures is becoming commonplace in the semiconductor industry. To ensure alignment between the different layers, the bottom-up technique of area-selective deposition (ASD) is promising. However, ASD may not always be feasible depending on the various surface chemistries present during manufacturing of complex semiconductor devices. Topographically selective deposition (TSD) is emerging as an alternative, focusing on differences in surface orientation rather than chemical properties. This work demonstrates a TSD supercycle approach in which atomic layer deposition (ALD) is directed to proceed exclusively within a 3D trench structure, by covering the top of the trench with an amorphous carbon (aC) inhibition layer. The aC layer is applied selectively on the top surface of the trench by exploiting the ion-radical synergy required for its deposition. Since the aC layer lacks adsorption sites for ALD precursors, growth of the target material is inhibited on the top surface of the trench, whereas it occurs selectively within the trench. After several ALD cycles of selective deposition of the target material, the aC layer is removed and reapplied in a supercycle recipe until sufficient material has been deposited in the trench. The selective deposition of an aC inhibition layer on the top surface of the trench, as well as the selective deposition of 3.0 ± 0.1 nm of TiO_2 in a trench is demonstrated on a 3D nanostructure.

In recent years, semiconductor architectures have undergone a shift from traditional planar architectures to 3D device structures to keep up with the demand for more advanced chips.[1] As 2D scaling of the devices is becoming less feasible, stacking the devices has emerged as a convenient strategy for increasing the number of devices on a given area.[2,3] Stacking devices does come with a new set of manufacturing challenges, particularly when it comes to the alignment of the features at different levels of the 3D structure. As a result of these developments, bottom-up processing techniques have been attracting attention due to their ability to enable self-aligned processing schemes.[4] One of the key bottom-up processing methods that is considered vital for semiconductor fabrication is area-selective deposition (ASD).[5] In ASD, the deposition of new material is directed to specific surfaces (the growth area), while other surfaces (the non-growth areas) are kept clear of any deposition. Typically, ASD is achieved through exploiting the differences in chemical character of the materials, which

comprise the growth and non-growth areas.[5] However, in the fabrication of advanced 3D structured devices, there may be too many different materials present, or the chemical differences are sometimes too small to be exploited, such that directing deposition through ASD is no longer feasible. As an alternative, topographically selective deposition (TSD) is being developed to expand the atomic-scale processing toolbox and aid in the fabrication of 3D structured devices.[6–11] For TSD, it is the orientation and location of surfaces in a 3D structure that dictate where deposition of the new material takes place, rather than their chemical character. Commonly, TSD is considered to be selective deposition on either horizontally or vertically oriented surfaces (h-TSD, v-TSD).

There are several approaches through which it is possible to arrive at 3D structures where material has been applied only on a specific orientation or location of the structure. Presently, the methods for achieving TSD can be divided in two categories: (1) methods where
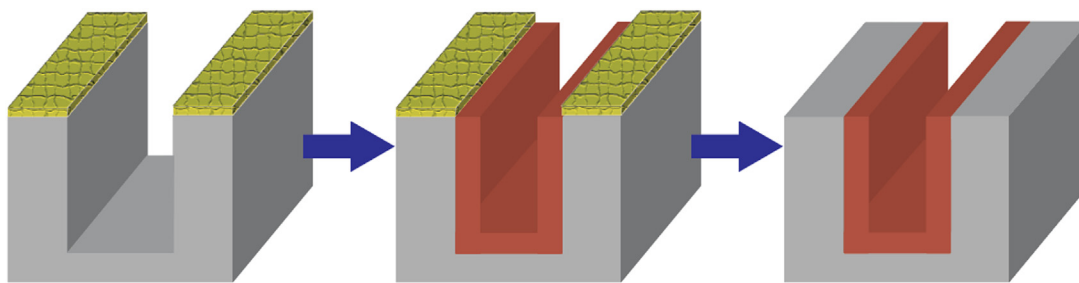
FIG. 1. The trench-only TSD method: first an aC inhibition layer is selectively applied on the horizontal top surface of a trench, as this is the only surface in the 3D structure where sufficient ions and radicals are present to facilitate the synergy required for its deposition. With the aC layer in place, ALD of a target material—TiO$_2$ in this work—takes place within the trench. Finally, the aC layer is removed resulting in the trench-only TSD structure.

material is deposited everywhere on a 3D structure and is subsequently selectively removed with anisotropic etching steps[6–8] and (2) methods where the materials are directly deposited in a topographically selective manner.[11] Both approaches have in common that they rely on exploiting the directional nature of ion bombardment from a plasma, as this allows for the horizontally and vertically oriented surfaces to be distinguished.

In the first category, material is selectively etched from horizontal surfaces, which then results in structures equivalent to v-TSD.[6–8] These anisotropic etching steps occur through sputtering, such as in the work of Chaker *et al.*[6] and Faraz *et al.*,[8] or by performing anisotropic atomic layer etching (ALE), as demonstrated by Jaffal *et al.*[7] In a related approach, ion bombardment during the deposition is employed to selectively modify the properties of the material in a topographically selective manner, thus creating a difference in etch rates between the material present on the horizontally and vertically oriented surfaces. Both Faraz *et al.*[9] and Vallée *et al.*[10] demonstrated that through this approach, it is possible to enable selective removal of the modified material. In the second category, the deposition of new material is directed to occur selectively on either a horizontally or vertically oriented surface. For example, Kim *et al.* demonstrated that a CF$_x$ film prepared by ion implantation can be employed to deactivate horizontally oriented surfaces toward atomic layer deposition (ALD), which allows for topographically selective deposition to proceed on the vertically oriented sidewalls.[11]

In this work, we introduce a trench-only TSD method that also belongs to the second category, as we utilize an amorphous carbon (aC) layer to selectively deactivate the horizontally oriented top surface, directing the deposition to proceed selectively at the bottom and on the sidewalls of a trench structure. The trench-only TSD process can have useful applications in the semiconductor industry for various situations where thin films are required exclusively within trench structures, such as for trench capacitors[12] and trench gates.[13] A schematic overview of the trench-only TSD approach is presented in Fig. 1.

Similar to the CF$_x$ film used by Kim *et al.*,[11] aC is capable of inhibiting ALD due to the absence of suitable adsorption sites for the precursors on the hydrocarbon surface. Both Zyulkov *et al.*[14] and Stevens *et al.*[15] demonstrated that aC can be effectively utilized as a non-growth area in an ASD context, in particular when an H$_2$ plasma treatment is applied to the aC surface to further passivate its surface. The aC layer used in this work is likewise able to block precursor adsorption. An example of inhibition of TiO$_2$ ALD is provided in

Fig. 2. The TiO$_2$ ALD recipe used in this work consisted of a 1.5 s TDMAT dose with a 10 s pump down step, followed by a 20 ms H$_2$O dose with a 32 s pump down step.[16] Saturation curves are given in the supplementary material.

Deposition of the aC inhibition layer proceeds only at the horizontal top surface of the trench, as we exploit the ion-radical synergy, which is critical for efficient aC deposition for the chemistry used. Because we utilize an Ar/CH$_4$ plasma in a pulsed plasma-enhanced chemical vapor deposition (PE-CVD) scheme, the ion bombardment is a key enabling factor for the aC growth.[17] The ion bombardment generates dangling bonds on the aC surface,[18] on which the sticking probability of the methyl radicals is much larger than on the hydrogenated sites on the aC surface.[19,20] Thus, aC deposition can take place when a surface is exposed to sufficiently high fluxes of both ions and methyl radicals. Due to the lack of ion bombardment on the sidewalls of the trench, aC deposition does not occur there. At the bottom of the trench, it is the lower flux of both methyl radicals and ions that keeps this area clear of aC. While relying on ion bombardment to address the horizontal surfaces separately from the vertical surfaces, the synergy required for effective deposition of the aC layer thus also allows for distinguishing between the top and bottom of a 3D structure. Even
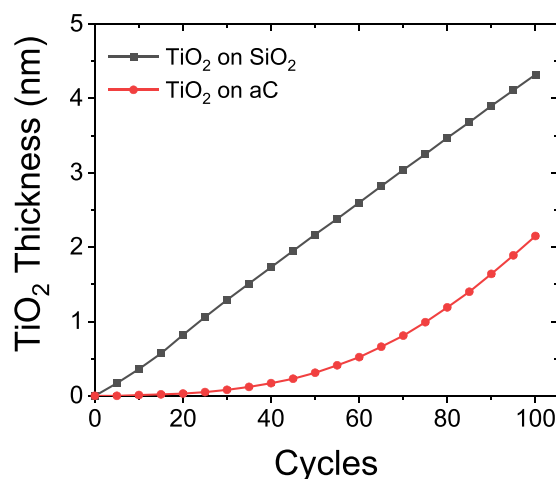

FIG. 2. Nucleation delay of TiO$_2$ on aC, which has received an H$_2$ plasma pretreatment. Selectivity above 90% is maintained for 20 ALD cycles, corresponding to 0.8 nm of selective TiO$_2$ growth on a SiO$_2$ substrate.

though dangling bonds are key for the growth of the aC layer, they are suspected to act as nucleation sites for ALD.[14,15] Hence, an H_2 plasma exposure is included in the process as a passivating step.

The presented TSD strategy involves a supercycle approach: when several ALD cycles of the target material have been performed, defects, i.e., TiO_2 nuclei, are starting to form, as evident from Fig. 2. To suppress the deposition of TiO_2 on the top of the trench, the aC layer was removed by an O_2 plasma, after which the TSD supercycle was restarted. Ultimately, this means the supercycle can thus be repeated until sufficient material has been deposited selectively. Based on these steps, a TSD supercycle recipe was developed for which an overview is given in Fig. 3.

Each TSD supercycle included 10 TiO_2 ALD cycles and this supercycle was repeated 12 times. The process was monitored with *in situ* spectroscopic ellipsometry of which the results are presented in Fig. 4. The thickness of the aC layer is modeled by a b-spline parametrization based on polyethylene. For the deposition of the TiO_2 on the aC inhibition layer, the same b-spline model is applied for simplicity. Finally, to model the accumulation of TiO_2 after the aC removal, a TiO_2 Cauchy model is utilized. The ellipsometry measurements were performed on a planar thermal SiO_2 sample, which was placed next to a 3D nanostructured sample in the reactor.

From Fig. 4, we find that the aC deposition rate is 0.082 ± 0.003 nm per PE-CVD cycle, producing an 8.2 ± 0.2 nm thick aC layer during each supercycle. The H_2 plasma treatment used to extend the nucleation delay[14,15] also slightly etches the aC inhibition layer at a rate of 0.028 ± 0.005 nm/s, yielding an aC layer of 6.84 ± 0.05 nm. Finally, during each O_2 plasma treatment, the aC is etched away with a rate of 0.49 ± 0.01 nm/s, meaning that most of the aC is already removed within the first 10 s of plasma treatment. After the O_2 plasma step of each supercycle, the TiO_2 defects that formed on the aC accumulate on the horizontal surfaces. This buildup of TiO_2 defects results in the presence of 0.10 ± 0.02 nm of TiO_2 after the 12 supercycles have completed.

As mentioned above, the supercycle process was performed on a 3D nanostructured sample, of which cross sections have been made for transmission electron microscopy (TEM) analysis as presented in Fig. 5. Figures 5(a) and 5(b) display bright field scanning TEM (BF-
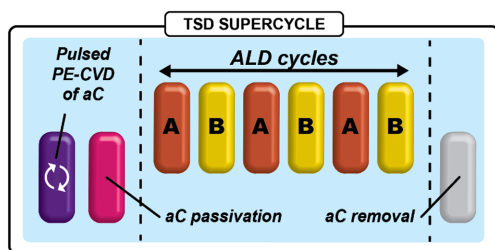

FIG. 4. The thickness of the aC and TiO_2 present on the horizontal surfaces as measured by spectroscopic ellipsometry. Irregular datapoints in supercycle 4 and 5 were caused by poor matching of the plasma as discussed in the supplementary material.

STEM) and complementary energy dispersive x-ray spectroscopy (EDS) elemental mappings of a cross section where only the aC layer was deposited. The image confirms that the aC layer is indeed deposited primarily on top of the trench structure. From the fact that the aC layer does not appear to grow as easily on the sidewalls of the trench, it can be concluded that both ions and radicals are required to enable the aC film growth. Figures 5(c) and 5(d) display a cross section of a sample where the full TSD process was conducted. The developed trench-only TSD process is effective in depositing the TiO_2 selectively on those surfaces that have not been covered by the aC layer. There has been significant deposition of TiO_2 on the sidewalls and the bottom of

FIG. 3. At the start of the TSD supercycle, the aC deposition is performed through 100 cycles of a pulsed PE-CVD process, described in detail in the supplementary material. After the aC deposition, a H_2 plasma (0.22 mbar; 200 ± 15 W) treatment is performed for 50 s, to passivate the aC and improve the achievable nucleation delay.[14,15] Next, the TiO_2 ALD is performed with (A) tetrakis(dimethylamino)titanium (TDMAT) as the precursor and (B) H_2O as the co-reactant. The last part of the TSD supercycle is the O_2 plasma (0.02 mbar, 200 W) applied for 50 s for the removal of the aC layer. The entire TSD supercycle proceeds at a substrate temperature of 110 °C.
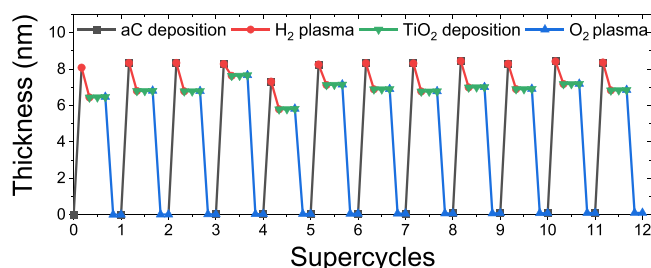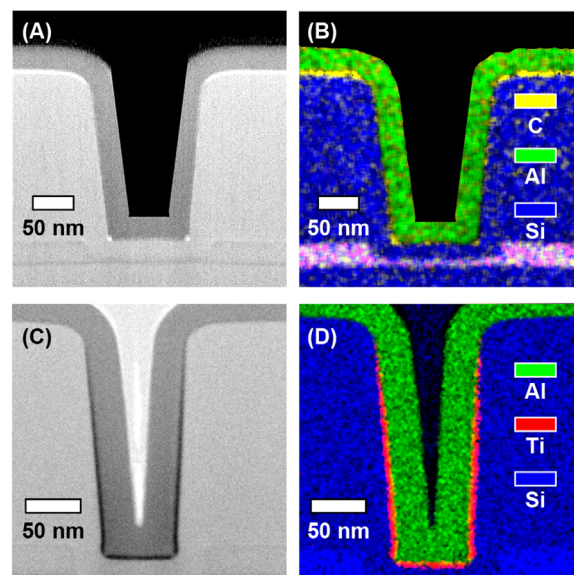

FIG. 5. BF-STEM images and complementary EDS elemental mappings of cross sections of 3D nanostructures with aspect ratios of [(a) and (b)] 1.6 and [(c) and (d)] 2.6, upon which the TSD process has been performed. For images (a) and (b), 100 cycles of the aC PE-CVD were performed, followed by the H_2 plasma treatment. For images (c) and (d), the entire TSD process, involving 120 TiO_2 ALD cycles was performed. Also, the TSD aC layer has been removed at the end of the process. Both samples were capped with 30 nm of Al_2O_3 to preserve the relevant interfaces during the fabrication of the cross section for the TEM study. Images (a) and (b) have been modified by masking off the capping layer for clarity. Unaltered versions are provided in the supplementary material.

the trench, whereas on the top of the trench no TiO_2 can be detected. At the bottom and the sidewalls of the trench, 3.0 ± 0.1 nm of TiO_2 is deposited, which tapers off nearer to the opening of the trench. It is likely that the incline of the trench sidewall enables some aC to be deposited here, which can impede the TiO_2 deposition. Similarly, some aC could have been deposited in the corners of the bottom of the trench, leading to discontinuity in the TiO_2 layer. Comparing the 3.0 ± 0.1 nm measured in the trench to the 0.10 ± 0.02 nm measured on the horizontal top surface, we can conclude that the complete TSD process has been performed with a selectivity of 94%.

In conclusion, we have demonstrated that by utilization of an aC inhibition layer, it is possible to selectively deactivate surfaces based on their orientation within a 3D structure. Specifically with the trench-only TSD supercycle we developed, the top surfaces of a trench can be selectively covered with aC, which then results in ALD proceeding selectively on the sidewalls and at the bottom of the trench. Because the deposition of the aC layer is restricted to the top of the trench due to flux limitations within the trench, it is reasonable to expect that the presented trench-only TSD process should be applicable to high aspect ratio trenches and vias as well. As the trench opening becomes narrower, the flux of species required for aC deposition would be limited even further, meaning that the deposition of the aC layer would become even more selective. Reducing the tapering of sidewalls (i.e., having more vertical sidewalls) should also ensure that the aC deposition is restricted to the top of the trench. The approach is expected to work independent of the critical dimension of the trench opening (for aspect ratios ≥ 1.6) and for different layer thicknesses. Furthermore, because selective deposition is achieved due to the inertness of aC layer toward the ALD chemistry, the developed supercycle would likely allow for the deposition of diverse materials in a topographically selective manner, making this a versatile approach for trench-only TSD.

See the supplementary material for a more in-depth description of the aC deposition method and the equipment utilized for this work. Also, we provide the saturation curves of the TiO_2 ALD process and a more detailed discussion on the datapoints of Fig. 4, as well as unaltered images of Fig. 5.

AUTHOR DECLARATIONS
Conflict of Interest

The authors have no conflicts to disclose.

Author Contributions

Thijs Janssen: Conceptualization (equal); Data curation (lead); Formal analysis (lead); Investigation (lead); Methodology (equal); Visualization (lead); Writing – original draft (lead); Writing – review & editing (equal). **Lodewijk J. P. Vossen:** Investigation (supporting).
Marcel A. Verheijen: Formal analysis (supporting); Investigation (supporting); Visualization (supporting); Writing – review & editing (supporting). **Wilhelmus M. M. Kessels:** Resources (equal); Supervision (supporting); Writing – review & editing (supporting). **Adriaan J. M. Mackus:** Conceptualization (equal); Funding acquisition (lead); Methodology (equal); Project administration (lead); Resources (equal); Supervision (lead); Writing – review & editing (equal).

DATA AVAILABILITY

The data that support the findings of this study are available from the corresponding author upon reasonable request.

REFERENCES

[1]H. H. Radamson, Y. Zhang, X. He, H. Cui, J. Li, J. Xiang, J. Liu, S. Gu, and G. Wang, "The challenges of advanced CMOS process from 2D to 3D," Appl. Sci. **7**(10), 1047 (2017).

[2]S. S. Kim, S. K. Yong, W. Kim, S. Kang, H. W. Park, K. J. Yoon, D. S. Sheen, S. Lee, and C. S. Hwang, "Review of semiconductor flash memory devices for material and process issues," Adv. Mater. **35**(43), 1–22 (2023).

[3]P. Ramm, A. Klumpp, J. Weber, N. Lietaer, M. Taklo, W. De Raedt, T. Fritzsch, and P. Couderc, "3D integration technology: Status and application development," in *36th European Solid State Circuits Conference (ESSCIRC 2010)* (IEEE, 2010), pp. 9–16.

[4]R. Clark, K. Tapily, K. H. Yu, T. Hakamata, S. Consiglio, D. O'Meara, C. Wajda, J. Smith, and G. Leusink, "Perspective: New process technologies required for future devices and scaling," APL Mater. **6**(5), 058203 (2018).

[5]G. N. Parsons and R. D. Clark, "Area-selective deposition: Fundamentals, applications, and future outlook," Chem. Mater. **32**(12), 4920–4953 (2020).

[6]A. Chaker, C. Vallee, V. Pesce, S. Belahcen, R. Vallat, R. Gassilloud, N. Posseme, M. Bonvalot, and A. Bsiesy, "Topographically selective deposition," Appl. Phys. Lett. **114**(4), 043101 (2019).

[7]M. Jaffal, T. Yeghoyan, G. Lefèvre, R. Gassilloud, N. Possémé, C. Vallée, and M. Bonvalot, "Topographical selective deposition: A comparison between plasma-enhanced atomic layer deposition/sputtering and plasma-enhanced atomic layer deposition/quasi-atomic layer etching approaches," J. Vac. Sci. Technol. A **39**(3), 030402 (2021).

[8]T. Faraz, Y. G. P. Verstappen, M. A. Verheijen, N. J. Chittock, J. E. Lopez, E. Heijdra, W. J. H. Van Gennip, W. M. M. Kessels, and A. J. M. MacKus, "Precise ion energy control with tailored waveform biasing for atomic scale processing," J. Appl. Phys. **128**(21), 213301 (2020).

[9]C. Vallée, M. Bonvalot, S. Belahcen, T. Yeghoyan, M. Jaffal, R. Vallat, A. Chaker, G. Lefèvre, S. David, A. Bsiesy, N. Possémé, R. Gassilloud, and A. Granier, "Plasma deposition—Impact of ions in plasma enhanced chemical vapor deposition, plasma enhanced atomic layer deposition, and applications to area selective deposition," J. Vac. Sci. Technol. A **38**(3), 033007 (2020).

[10]T. Faraz, H. C. M. Knoops, M. A. Verheijen, C. A. A. Van Helvoirt, S. Karwal, A. Sharma, V. Beladiya, A. Szeghalmi, D. M. Hausmann, J. Henri, M. Creatore, and W. M. M. Kessels, "Tuning material properties of oxides and nitrides by substrate biasing during plasma-enhanced atomic layer deposition on planar and 3D substrate topographies," ACS Appl. Mater. Interfaces **10**(15), 13158–13180 (2018).

[11]W. H. Kim, F. S. Minaye Hashemi, A. J. M. Mackus, J. Singh, Y. Kim, D. Bobb-Semple, Y. Fan, T. Kaufman-Osborn, L. Godet, and S. F. Bent, "A process for topographically selective deposition on 3D nanostructures by ion implantation," ACS Nano **10**(4), 4451–4458 (2016).

[12]Z. Hu, Q. Zhou, H. Ma, M. Wang, Y. Zhong, and Y. Dou, "Development of low cost glass-based deep trench capacitor for 3D packaging," IEEE Electron Device Lett. **44**(9), 1535–1538 (2023).

[13]X. Chen, F. Li, and H. L. Hess, "Trench gate β-Ga_2O_3 MOSFETs: A review," Eng. Res. Express **5**, 012004 (2023).

[14]E. Stevens, Y. Tomczak, B. T. Chan, E. Altamirano Sanchez, G. N. Parsons, and A. Delabie, "Area-selective atomic layer deposition of TiN, TiO_2, and HfO_2 on silicon nitride with inhibition on amorphous carbon," Chem. Mater. **30**(10), 3223–3232 (2018).

[15]I. Zyulkov, E. Voronina, M. Krishtab, D. Voloshin, B. T. Chan, Y. Mankelevich, T. Rakhimova, S. Armini, and S. De Gendt, "Area-selective Ru ALD by amorphous carbon modification using H plasma: From atomistic modeling to full wafer process integration," Mater. Adv. **1**(8), 3049–3057 (2020).

[16]Q. Xie, Y. L. Jiang, C. Detavernier, D. Deduytsche, R. L. Van Meirhaeghe, G. P. Ru, B. Z. Li, and X. P. Qu, "Atomic layer deposition of TiO_2 from tetrakis-dimethyl-amido titanium or Ti isopropoxide precursors and H_2O," J. Appl. Phys. **102**(8), 083521 (2007).

[17]A. Von Keudell and W. Jacob, "Elementary processes in plasma-surface interaction: H-atom and ion-induced chemisorption of methyl on hydrocarbon film surfaces," Prog. Surf. Sci. **76**(1–2), 21–54 (2004).

[18]H. Sugiura, H. Kondo, T. Tsutsumi, K. Ishikawa, and M. Hori, "Effects of ion bombardment energy flux on chemical compositions and structures of hydrogenated amorphous carbon films grown by a radical-injection plasma-enhanced chemical vapor deposition," J. Carbon Res. **5**(1), 8 (2019).

[19]A. Von Keudell, T. Schwarz-Selinger, M. Meier, and W. Jacob, "Direct identification of the synergism between methyl radicals and atomic hydrogen during growth of amorphous hydrogenated carbon films," Appl. Phys. Lett. **76**(6), 676–678 (2000).

[20]P. Träskelin, E. Salonen, K. Nordlund, J. Keinonen, and C. H. Wu, "Molecular dynamics simulations of CH_3 sticking on carbon surfaces, angular and energy dependence," J. Nucl. Mater. **334**(1), 65–70 (2004).